Barnes, N., A. F. Scott, P. Lieby, M. A. Petoe, C. McCarthy, A. Stacey, L. N. Ayton, N. C. Sinclair, M. N. Shivdasani, N. H. Lovell, H. J. McDermott, and J. G. Walker. 2016. Vision function testing for a suprachoroidal retinal prosthesis: effects of image filtering. *Journal of Neural Engineering*. **13**(3): 036013.

doi: https://doi.org/10.1088/1741-2560/13/3/036013

Vision function testing for a suprachoroidal retinal prosthesis: effects of image filtering

Nick Barnes[1,2*], Adele F Scott[1], Paulette Lieby[1], Matthew A Petoe[4,6], Chris McCarthy[1,2,7], Ashley Stacey[1], Lauren N Ayton[5], Nicholas C Sinclair[4], Mohit N Shivdasani[4,6], Nigel H Lovell[8], Hugh J McDermott[4,6], Janine G Walker[1,3] and for the BVA Consortium

Abstract

Objective. One strategy to improve the effectiveness of prosthetic vision devices is to process incoming images to ensure that key information can be perceived by the user. This paper presents the first comprehensive results of vision function testing for a suprachoroidal retinal prosthetic device utilizing of 20 stimulating electrodes. Further, we investigate whether using image filtering can improve results on a light localization task for implanted participants compared to minimal vision processing. No controlled implanted participant studies have yet investigated whether vision processing methods that are not task-specific can lead to improved results. *Approach.* Three participants with profound vision loss from retinitis pigmentosa were implanted with a suprachoroidal retinal prosthesis. All three completed multiple trials of a light localization test, and one participant completed multiple trials of acuity tests. The visual representations used were: Lanczos2 (a high quality Nyquist bandlimited downsampling filter); Minimal Vision Processing (MVP); Wide View regional averaging filtering (WV); scrambled; and, system off. *Main Results.* Using Lanczos2, all three participants successfully completed a light localization task and obtained a significantly higher percentage of correct responses than using MVP ($p \leq 0.025$) or with system off ($p < 0.0001$). Further, in a preliminary result using Lanczos2, one participant successfully completed grating acuity and Landolt C tasks, and showed significantly better performance ($p = 0.004$) compared to WV, scrambled and system off on the grating acuity task. *Significance.* Participants successfully completed vision tasks using a 20 electrode suprachoroidal retinal prosthesis. Vision processing with a Nyquist bandlimited image filter has shown an advantage for a light localization task. This result suggests that this and targeted, more advanced vision processing schemes may become important components of retinal prostheses to enhance performance. ClinicalTrials.gov Identifier: NCT01503576.

1 Introduction

Prosthetic vision is a promising approach for restoring rudimentary visual percepts to individuals with profound visual impairment. A number of implantable devices have been pursued to elicit visual percepts by electrically stimulating intact residual neurons of the visual system, including the retina, [1, 2, 3, 4, 5, 6], optic nerve [7, 8] lateral geniculate nucleus [9, 10], and visual cortex [11]. Other approaches have also been proposed (e.g., [12]). Multi-center studies have shown results on a 60 electrode epi-retinal implant by Second Sight Medical Products [1], and a 1500 micro-photodiode subretinal implant by Retinal Implant AG [13]. Recent or current chronic human implant trials have been conducted by Pixium (www.clinicaltrials.gov, trial #NCT01864486), and Bionic Vision Australia [14].

Epiretinal and subretinal implants have shown successful results in vision testing trials. For example, vision function studies have reported successful completion of basic low vision tests (e.g., [1, 13]), and best acuity of 1.8 LogMAR [1] and 1.43 LogMAR [13]. Functional vision results reported include letter reading [2], object localization and identification [13], and mobility tasks [1]. This paper is the first comprehensive report of implanted participant vision testing using a suprachoroidal retinal prosthetic device.

Prosthetic vision uses an image sensor to capture visual data, such as eye-resident micro-photodiodes [13] or a head-mounted camera [1]. Sensors optically blur, then spatially integrate incoming light over the area of each photosensitive pixel, forming the sensor's point spread function (PSF) [15]. We define vision processing as hardware or software operations that transform visual data from the sensor to perceptual parameters that are coded as stimulation. Vision processing is a promising approach to improving patient outcomes. A broad range of devices can apply vision processing, regardless of the limitations of number of electrodes and dynamic range.

Many image enhancement techniques have been proposed for impaired vision, with some evaluated with low vision participants (e.g., [16, 17, 18, 19]). Some studies show benefit. For example, adaptive filtering and thresholding can improve face recognition [16], augmenting contours can improve search time [17]. Other studies report a preference for an enhancement (e.g., [18, 19]). There are no reports these methods being used for vision processing

*Correspondence: nick.barnes@nicta.com.au
[1]NICTA Computer Vision Research Group, Building A, 7 London Circuit, Canberra, Australia
[2]Research School of Engineering, Australian National University
Full list of author information is available at the end of the article

in implanted retinal prosthetic patient trials; however, these techniques may be good candidates for such use.

Some of the image enhancement techniques proposed for implantable prosthetic vision have shown promising results in evaluations using simulated prosthetic vision (SPV) with normally-sighted participants [20]. These include image filtering [21, 22, 23, 24], saliency [25], and prosthetic face fixation [26]. Weiland *et al.* [27] evaluated a tactile assistance system for obstacle avoidance with visually-impaired subjects. McCarthy *et al.* [28] investigated augmenting a prosthetic vision visualization to make low-contrast obstacles evident. Eckmiller *et al.* [29] presented a "road map" for a retina encoder to learn parameters of image filters to map to stimulation, and evaluated dialog-based tuning using SPV. SPV has also been used to investigate how prosthesis design may affect performance on particular tasks, including acuity [30, 31, 22], tracking [23], mobility [32], and face and object recognition [33, 34].

In normal human vision, diffraction through a nominal 2 *mm* diameter pupil aperture performs approximately Nyquist bandlimited filtering with respect to peak foveal photoreceptor density [35]. SPV studies have investigated image filtering for downsampling. Hayes *et al.* [31] used regional averaging, also referred to as box filtering [34] or circular averaging [22]. Using circular averaging, Chen *et al.* [22] explored image sampling geometries and filter size. Hallum *et al.* [23] showed that for a target pursuit task, participants performed significantly more accurately using a Gaussian filter than using regional averaging or impulse sampling. Further, saccade end-point accuracy was significantly more accurate when using Gaussian filtering or regional averaging than when using using impulse sampling. Theoretical analysis showed that Gaussian filtering better reduces the uncertainty in tracking target position [36].

Despite SPV studies showing that higher quality filters improve results [23], to our knowledge, no controlled implanted participant studies of image filters for downsampling have been conducted. Humayun *et al.* report that options for image filters are available to users, but do not specify what was used in their human trials [37]. Further, despite many methods proposed and evaluated in low vision and SPV, no controlled study has shown benefits of a vision processing technique that is suitable for a wide range of tasks. Improvements have been shown for face detection [38], but the vision processing used was specialized for that task. An investigation of vision processing to improve acuity also included user-controlled zooming [39]. In reported implanted participant studies: (1) there is little focus on vision processing; (2) vision processing methods that are employed are not fully specified; and (3) vision processing investigated in controlled studies incorporated manual steps or are applicable only to a narrow range of tasks.

Filtering for downsampling is well-understood in signal processing. A bandlimited signal (containing only frequency components below a threshold frequency) is uniquely determined by samples at least twice the rate of the highest frequency component [40]. A Nyquist bandlimited filter, that removes all frequencies greater than the Nyquist frequency and retains all below, can be used for theoretically ideal downsampling [40]. For image processing, the normalized sinc function is the spatial equivalent of the ideal downsampling filter [40], but causes ringing [41]. Filters that approximate the normalized sinc function [40, 42] have good properties, specifically: retaining image sharpness; reducing aliasing; and, reducing or eliminating ringing. As such they are commonly used in graphics, and signal and image processing. Lanczos filters are of this type and are among the best performing image filters [42].

Participant	P1	P2	P3
Age in Years	52	49	63
Sex	Female	Male	Male
Eye Condition	RP (Rod-Cone Dystrophy)	RP (Bardet-Beidl Syndrome) Nystagmus	RP (Rod-Cone Dystrophy) Nystagmus
Years of Light Perception Vision	20	10	20
Usual Mobility Assistive Device	Guide dog	Guide dog	Guide dog

Note. RP - Retinitis Pigmentosa.

Table 1: Participant characteristics of recipients of the suprachoroidal retinal prosthesis.

In this paper, we present the first comprehensive report of vision function testing of a 20 stimulating electrode suprachoroidal retinal prosthesis (summary findings were presented in [14]). Further, for the first time in implanted participant studies, we investigate how different image filters affect vision test results. Image filtering is a basic operation, and perhaps an obvious component of a retinal prosthetic. Certainly, we anticipate that more sophisticated approaches will be used to process incoming images. However, high quality filtering is a general processing that applies to many tasks, and is a basic underlying component of other vision processing methods (e.g., [16, 29]).

2 Methods and Materials

2.1 Participants, Screening and Recruitment

A suprachoroidal retinal prosthesis was surgically implanted in three participants with profound vision loss from retinitis pigmentosa (i.e., bare-light perception in both eyes) from May to August 2012. Data collection pertaining to the light localization and visual acuity tasks described below occurred between August 2013 to June 2014. The implant trial was completed in August 2014. The Human

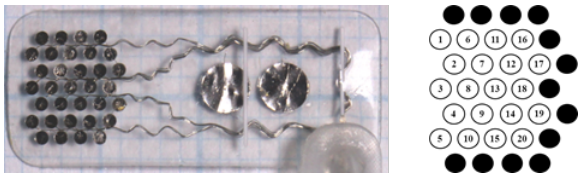

Figure 1: The intraocular electrode array comprises a silicone substrate (19 *mm* long, 8 *mm* wide) with 33 platinum stimulating electrodes (30 x 600 μm, 3 x 400 μm), and 2 large return electrodes (2000 μm). The outer ring of electrodes (shown in black, right) was connected together to form a "guard ring" return electrode. Stimulating electrodes were arranged in a hexagonal configuration, with uniform distance of 1mm between neighboring electrode centroids.

Research Ethics Committee at the Royal Victorian Eye and Ear Hospital, Australia approved the study. All participants provided written informed consent after being provided with electronic and audio versions of the project information. The study was registered at www.clinicaltrials.gov (Identifier Number: NCT01603576) and adhered to the tenets of the Declaration of Helsinki. The recruitment and screening procedures as well as the inclusion and exclusion criterion are described in detail in [14]. Relevant characteristics of the three participants can be seen in [43] and are summarized in Table 1.

2.2 The Suprachoroidal Retinal Prosthesis

The retinal prosthesis used in this study consists of an intraocular electrode array, composed of a silicone substrate (19 *mm* long, 8 *mm* wide) with 33 platinum stimulating electrodes (30 x 600 μm, 3 x 400 μm) and two large return electrodes (2000 μm), similar to the preclinical array described previously (Figure 1) [44]. It was implanted into the suprachoroidal space using novel surgical procedures developed by our team [45]. The inner 4 x 5 array of electrodes could be individually stimulated. These had a uniform distance of 1 *mm* between all neighboring elements, with centers covering 3.5 *mm* x 3.46 *mm* (Figure 1).

2.3 External Processing

Participants wore a small front-facing camera mounted on a pair of glasses (Scene Camera, Arrington Research Inc., AZ). Images captured by this camera were processed on a standard laptop computer. Vision processing was performed using Matlab (Mathworks, MA) running under Windows XP, resulting in stimulation parameters being set for each electrode. These stimulation parameters were communicated to a custom-built stimulator (neuroBi Bionics Institute, Australia [46]) as a serial sequence, which triggered stimulus delivery directly to the implanted electrodes via a percutaneous connection.

Percepts with controllable brightness can result in response to stimulation on a single electrode [47]. These percepts are often referred to as phosphenes. Vision processing requires a map to specify the location in the input image from which the visual data will be taken that will determine the stimulation parameters that induce a phosphene. Human retinal implant studies to date that stimulate based on visual sensor data typically map directly from the input visual space corresponding to the retinal position of the electrode being stimulated [1, 13]. Note that other approaches have been proposed for use in determining this map, including phopshene maps and the retinal encoder. A phosphene map, a map of perceived phosphene locations, can be determined behaviourally using self-reported participant information [48]. The retinal encoder [29, 49] proposed that image filter parameters including such location mappings can be learned. However, there are no reports of these alternative methods being used for vision testing in implanted participant studies.

In this paper, we follow this typical approach for mapping input images. We apply a filter to a region of the image centered approximately corresponding to the retinal position of the stimulating electrode. The filter output is used to determine stimulation intensity. We refer to this image region as the visual field corresponding to that electrode.

The camera was placed so that when the participant was comfortably looking forward, the camera view corresponded approximately with phosphene locations. The field-of-view corresponding to the electrode centers was estimated to be 12.4° x 12.2° (i.e. approximately 3.5° / *mm*) [50]. In the case of Lanczos2 and WV, the visual fields for each electrode have a radius estimated as 7.0° and 3.5° respectively, leading to a total field-of-view that influences the phosphene values of 26.4° x 26.2 ° and 19.4° x 19.2°.

Electrical stimulation parameters were determined for each participant in a psychophysics setting to obtain clear and reliable phosphenes on all electrodes. These were generated in the form of a phosphene map for each participant which specified the number of available electrodes that could be used for stimulation. These were 20, 17 and 20 in Participants 1, 2 and 3 (P1, P2, and P3) respectively (see [51]). The electrical stimulation parameters for each electrode were: the pulse width; interphase gap and stimulation rate; threshold current and maximum current below the safe charge limit (447 *nC* for 600 μm diameter, 298 *nC* for 400 μm diameter based on data by Merrill *et al.* [52]. This equates to an upper limit of charge density of 158 μC/cm^2 and 237 μC/cm^2). For P3, ganged pairs of adjacent electrodes were used due to higher thresholds, hence 10 ganged pairs were made available from 20 individual electrodes. Variation between participants of the number of electrodes available for stimulation has also been reported in other studies (e.g., [1]).

Resulting stimulation output was interleaved using a single current source, delivering 50, 400, and 200 Hz for each

electrode for P1, P2 and P3, respectively. In retinal prostheses, it has been observed that if stimulation is continued for some time, an initially bright percept will fade, or that the percept will remain for some time after stimulation ceases [53, 54]. To alleviate such temporal variations, stimulation was interspersed with intervals of no stimulation. The cycle length of stimulation versus no-stimulation was set during piloting to ensure that each participant reliably observed stimulation activity; effectively a duty cycle function of 50% over 2, 5 and 4 seconds / electrode for P1, P2 and P3 respectively. However, in performing the gratings test, P1 appeared to be more sensitive to temporal issues, and so a 100% duty cycle was used with stimulation of 200 Hz, with a recovery period after each presentation.

2.4 Image Filters

To select filters for investigation, performance for downsampling and computational cost (which impacts battery life) were key considerations. Lanczos2, wide view circular regional averaging (WV) and impulse sampling were selected. Impulse sampling maps the value of only the nearest-neighbour input pixel to the corresponding output stimulation parameters. As this operation has low computational cost, we refer to it as minimal vision processing (MVP). The Lanczos family of filters are high performing image filters. They are computed as a weighted sum of pixels, and so have the same computational cost for a given filter size as many other similar or lesser performing filters (e.g., Gaussian). Circular regional averaging takes an arithmetic mean of pixels within a specified radius, a sum without weights. However, as multiplication by a fixed weight adds little or no computational cost on modern processors [55] [56], Lanczos2 and WV have similar computational cost for the same filter size. Typical optimizations such as windowing and separable filters do not apply in this case because the filter only needs to be evaluated once per visual field (stimulating electrode) per image.

Figure 2 shows comparative performance when different image filters are applied to every pixel of 2(a). Stimulation amplitude is set by mapping the result of applying a filter to the camera view location corresponding to an electrode. Figures 2(b-g) show the values that would be mapped if a head-mounted camera were moved to align an electrode with each pixel of (a). As expected Lanczos2 performs well, 2(b). As Lanczos2 has a larger filter size than Gaussian or regional averaging for a particular cut-off frequency, in Figure 2(c), we first decimate the image using a standard image pyramid approach so the filter size is approximately the same, resulting in little loss of output quality. Using circular regional averaging, 2(d,e), leads to blurring, and small features are less visible (the smaller circles fade considerably). With Gaussian, 2(f), the cut-off is less precise than for Lanczos2, leading either to over-filtering or aliasing. Finally, MVP results in significant aliasing (see 2(g)). The trial includes Lanczos2 as a high quality weighted filter, regional averaging as a popular choice in previous literature, and MVP. If constraints on battery life overwhelm performance considerations MVP should be used. However, whether MVP's reduced performance impacts participant results compared to a high quality image filter is a key question that we will address. Note for poor low-pass filters, such as circular averaging, cut-off is imprecise, and so can be set to favour aliasing reduction or sharpness (Figure 2(c) and (d) show alternative settings for regional averaging).

2.5 Vision Processing

Our experiments compared a total of five conditions: the proposed Nyquist bandlimited Lanczos2 filtering; MVP; WV; scrambled, and system off. Not all five conditions were included in each of the three experiments conducted. The experimental setting was such that when we compared Lanczos2 filtering with comparator vision processing methods, all other aspects of the research design and method were identical (e.g., stimulation, lighting, etc.).

All of the vision processing strategies (Lanczos2 filtering, MVP, WV and scrambled) operate on a grayscale input-image stream. For each strategy, the filter was applied to discrete video frames at the centroid of phosphene locations (corresponding to electrode positions). The filter output at each location was then mapped to the possible stimulation values of the corresponding electrode. The minimum non-zero output of the filter was assigned to the psychophysical threshold current for each electrode. The maximum value of the filter output was assigned to the maximum current for a particular electrode; i.e., up to 6dB above threshold and always within safe charge limits [52]. Output between these values was mapped linearly onto a dB scale. Zero output from the filter produced no stimulation.

2.5.1 The Nyquist Bandlimited Lanczos2 Filter

The Lanczos family of filters are normalized sinc functions in the spatial domain that are truncated symmetrically by multiplication with a rectangular window to have $n-1$ side lobes, then multiplied by another sinc function [57]. Figure 3(b) shows the Lanczos2 filter, where $n = 2$. Lanczos filters have good theoretical performance [57]. The Lanczos filter was in the group of windowed-sinc function filters that showed the most accurate results in a study of many downsampling filters [42], and performed best in terms of key properties in comparison to several other filters including regional averaging and Gaussian [58]. A single lobe of ringing (See Figure 3(b)), emphasising the centre with an outermost small negative lobe, has been observed to sharpen images [59]. This feature has led to popular use of Lanczos2 in image processing (see www.imagemagick.org/Usage/filter/.)

The filter size (the only parameter) was set to be Nyquist-bandlimiting with respect to the projected distance between

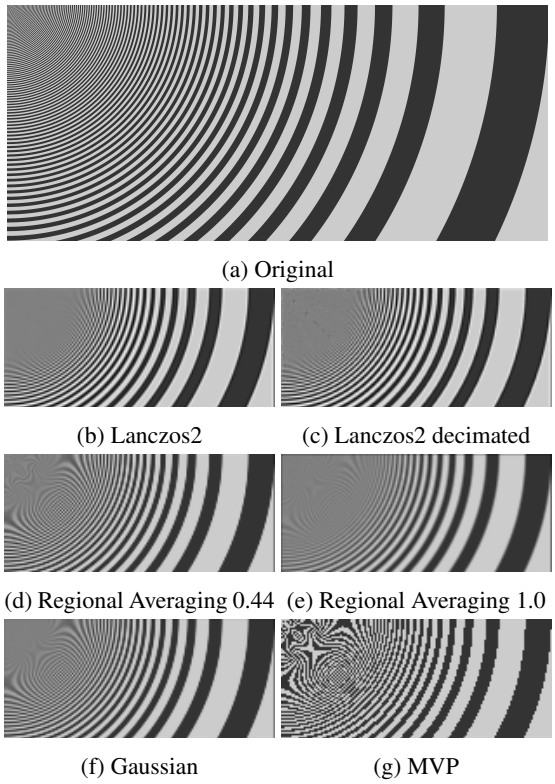

(a) Original

(b) Lanczos2 (c) Lanczos2 decimated

(d) Regional Averaging 0.44 (e) Regional Averaging 1.0

(f) Gaussian (g) MVP

Figure 2: A comparison of image filters for downsampling: (a) Input image. (b) Lanczos2 (Nyquist cut-off), top left of the image is largely grey, larger frequencies are retained, only a narrow transition region is grayed. (c) decimation to 0.25 before Lanczos2, shows little change. (d) circular averaging (width 0.44), retains lower frequencies and sharpness, but aliasing top left; (e) circular averaging (width 1.0, favouring aliasing reduction), fewer artefacts, but larger frequencies are attenuated (more circles greyed); (f) Gaussian (half power), similar to (d) but less artefacts. (g) MVP, shows strong aliasing.

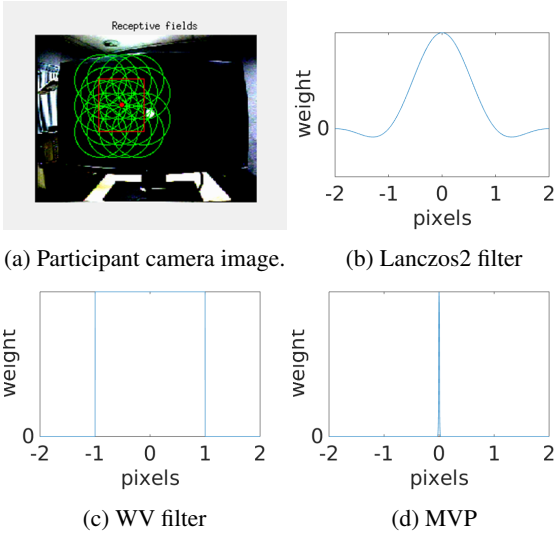

(a) Participant camera image. (b) Lanczos2 filter

(c) WV filter (d) MVP

Figure 3: (a) The green rings show the visual field for each electrode for the Nyquist bandlimited Lanczos2 filter. The red dot and square are the image center and estimated projection of the electrode centers respectively. Note that in the experiments, the background to the screen was covered in a dark color to reduce distractors. (b)-(d) show the spatial filters used and their weights. The units of the pixel axes are the interphosphene distance. (b) Center pixels are strongly weighted, reducing further away, with a small distant ring has negative weight. (c) Every pixel within a fixed radius (here, the interphosphene distance) has equal weight. (d) Only the nearest neighbor pixel value is used.

electrode centers. In a previous study using normally-sighted participants, we showed that setting the filter size of the Lanczos2 filter to be Nyquist bandlimiting or slightly smaller leads to improvements in acuity compared to setting the size at other values [24].

2.5.2 Minimal Vision Processing

It would be ideal to have a comparator of no vision processing. However, as the camera is connected to stimulation via a processor, some processing must take place to link the two. MVP is the minimal computational cost method for this operation, and so was used as a control method. MVP is similar to what would occur if an image filter, such as Lanczos2, were applied with a minimally narrow width.

In Hallum *et al.* [23], the simulation of impulse sampling had a limitation: pixels were binary only, and hence so was filter output. However, in general, with the PSF of a real camera, a pixel value on the boundary of an input stimulus will be a mixture of the two values.

2.5.3 Wide View Regional Averaging (WV)

WV can reduce aliasing compared to MVP, but has significantly higher computational cost. However, Smith [60] describes it as a poor low-pass filter, leading to loss of sharpness and aliasing. This control strategy was chosen as it is a typical approach in the literature [22, 23]. We set the filter radius to the projected distance between electrode centers, to block most energy from frequencies above the Nyquist limit and ensure a wide field-of-view. This gives a comparison of filtering that attenuates some frequencies beyond the Nyquist frequency.

2.5.4 System Off

No stimuli were delivered to the electrodes in the system off condition. The participants reported that no visual activity was apparent from the implant in all trials with the system switched off. The use of system off is standard in trials of implanted retinal prosthetics [1, 13], and is necessary to control for residual vision.

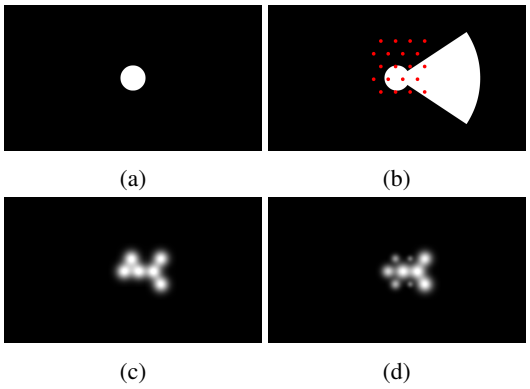

Figure 4: The BaLM Light Localization Task [63]. A fixation disc is the apex of a wedge having one of four directions: up down, left or right. (a) the central disc. (b) the central disc and left light wedge. The red dots show phosphene sampling positions. (c) phosphene activations that result when MVP is applied to (b). (d) phosphene activations that result when the Lanczos2 filter is applied to (b). Image filtering preserves shape and consistency when the viewpoint moves. Whereas in (c) activation is based on one pixel value, and so the result is subject to rapid change near a stimulus boundary.

2.5.5 Scrambled

As a participant may be able to infer that the system is switched off when there is no visual activity, studies sometimes include a scrambled mode (e.g., [61, 62]). In scrambled, electrode stimulation is computed from the image in the usual way (in our case Lanczos2 processing), but then assigned to random electrodes or phosphene locations. Thereby, stimulation is active and overall brightness is maintained, however, the spatial structure of video image is disrupted [62]. We changed the random assignment once each five seconds throughout the session. The same definition used for the Argus II in [61, 62] except that random assignment was performed once per participant session.

2.6 Stimulus, Task and Outcome Performance Measures

2.6.1 Localization of Light Task

Visual function was assessed for all three participants using the light localization task which was a sub-test in the Basic Assessment of Light, Location, Time and Motion Test Battery (BaLM) [63]. The light localization task measures an individual's ability to perceive the direction of a wedge of projected light using, in this case, a four-alternative-forced-choice (4AFC) scheme [63]. The wedges were randomly presented up, down, left, and right in relation to the central fixation disc as shown in Figure 4. The diameter of the initial fixation disc was 6°, with 20° eccentricity for the wedges relative to the viewing position.

The light localization stimuli were presented on a computer screen with 2048 x 1280 resolution (76.2 cm; Dell U3011), while participants were seated with a calibrated distance of 57 cm from their head-mounted camera to the computer screen. The wedges of light were presented against a black background with lighting conditions controlled. Ambient lighting was 111 lux, equivalent to a dimly-lit room. Measurement was made each session using an Amprobe LM-200LED light meter with the measuring transducer placed at the participant's head, facing up towards the lighting source.

The participants were asked to look at the middle of the screen which was facilitated using proprioceptive feedback by allowing them to touch the screen before the testing phase commenced. The presentation of the images was delivered by a researcher. Presentation of a randomly located light wedge occurred after the participant verbally indicated that they found the central fixation point. The researcher confirmed that the participant was fixated in the correct location using an eye tracking camera (Arrington Research Inc., AZ) for the first of each group of trials. Participants were allowed to scan with their head and no time limitations were imposed to give a response. Also, participants were not specifically instructed to keep their eyes fixated while performing head scanning. Responses were given verbally by participants, and recorded by two researchers on score sheets. Response time for each trial was captured for a subset of the trials using Matlab (Mathworks, MA). The participants completed eight training trials at the beginning of each session to familiarize themselves with the task. The stimuli were presented in blocks of eight trials with one vision processing method (Lanczos2, MVP or system off) used for each block. Response accuracy was recorded for each trial and defined as successfully describing the location the wedge of light. The chance rate of accuracy was 25%, and 62.5% was the criterion set as a benchmark for clinical meaningfulness, given that possible responses were within 4AFC [63]. Inter-rater reliability was excellent with 100% agreement for response accuracy. Figure 5 shows a photograph of a participant in the experimental setup for the light localization task.

Response time, i.e., self-paced trial time was determined as the time (seconds) from when the stimulus was presented to when the participant gave their verbal response.

2.6.2 Visual Acuity Tasks

Participants conducted acuity tasks, gratings and Landolt C optotypes.

Gratings Visual Acuity was measured using the relevant sub-test from the Freiburg Visual Acuity Test (FrACT; v. 3.8.1sq) [64, 65]. The participant was asked to identify the orientation of parallel lines of varying spacing from one of four possible alternative choices (4AFC). The best PEST (parameter estimation by sequential testing) method was

Figure 5: The experimental setting for the light localization task. The participant can be seen with the head-mounted camera directed towards the light localization fixation dot. Participants are free to move their head to scan with the camera. Investigators MP and CM are also visible.

used to determine the gratings acuity threshold [66]. Stimuli were presented as a 1280 x 800 resolution image onto a 2030 x 1520 *mm* projector screen (Grandview GRPC100V) using a ultra short throw projector (Dell S500wi). Gratings were square-wave filtered, and the optotype diameter was set to occupy the entire screen with the image dimension corresponding to 2.85 arcmin / pixel at a 2-meter viewing distance.

Electrode spacing on the retina gives a prediction of the acuity that could be achieved with a retinal prosthesis with the presentation of a static image. This provides a useful insight as to the limits of acuity for a particular device, We refer to this predicted acuity as the static theoretical expectation for the device. Results from the multi-centre studies show that a minority of participants can achieve better acuities, while most achieve worse [1, 13]. Better acuities may have been achieved by scanning the image. The static theoretical expected acuity for the suprachoroidal implant corresponded to a minimal grating distance of 0.141 cycles per degree [cpd; 2.33 logMAR; (20/4242)] as constrained by the 1 *mm* horizontal electrode spacing.

The participant completed a series of 24-trial blocks; however, the initial trial was discarded as the FrACT Grating Acuity task commences at a default setting of 0.48 cpd which is too small to resolve with the suprachoroidal retinal implant. To address this issue an incorrect response was purposefully selected for the first presentation (excluded from further analyses) which resulted in the first stimulus being presented to the participant at 0.121 cpd. The trial blocks allowed for a threshold search of visual acuity that comprised at least six reversals. The FrACT Grating Acuity test has been validated for individuals with low vision and used in research investigating the efficacy of vision assistive devices [64, 67, 68].

The participant was allowed to scan with their head and had unlimited time to respond. The responses were given verbally by the participant, and recorded by the researcher using a keypad linking to the FrACT software. Best PEST acuity threshold results, scores per presentation, and response times per presentation were recorded and analyzed for each of the vision processing methods (Lanczos2, MVP, WV, scrambled and system off).

Landolt C Optotype Visual Acuity was measured using the FrACT (v. 3.8.1) [64, 65]. P1 was asked to locate the gap in the "C" optotype from one of four possible orientations (4AFC; up, down, left, right). Similar to the gratings acuity task, a modified best PEST method with an adaptive staircase procedure was used to calculate the optotype acuity threshold. Stimuli were presented as a 1280 x 800 resolution image onto a 2030 x 1520 *mm* projector screen. The maximum diameter of C optotype was 800 pixels (38°), with a gap width of 160 pixels (7.6°). Due to a software limitation (floor effect) we were unable to estimate any visual acuity poorer than 3.24 logMAR. The participant was trained to find the center of each optotype by first judging its width and height. From this central fixation point, the participant explored regions in the four possible directions, by adjusting their head azimuth or elevation, returning to the center each time and repeating this process until ready to respond [14]. The participant completed a series of 12-trial blocks (with an additional three 24-trial blocks).

The participant was allowed to scan with their head and had unlimited time to respond. The responses were given verbally by the participant, and recorded by the researcher using a keypad linking to the FrACT software. Best PEST acuity threshold results (measured as logMAR units), and average response times for each trial block were recorded and analyzed for each of the vision processing methods (only Lanczos2, MVP and system off for this trial).

2.7 Study Design

The study had a within-subject repeated measure design that was randomised and controlled, that is, the order of presentation of the vision processing methods was counterbalanced, controlled and randomly allocated for each session using a computerized automated system. The study investigated potentially effective vision processing methods for enhancing performance on visual functioning tasks using Lanczos2 filtering, and a range of comparators (MVP, WV), as well as scrambled and system off. For the light localization task, P1 - P3 completed 4 - 5 weekly sessions in which they responded to 40 - 60 trials / session. Data was collected only from P1 for the gratings and Landolt C optotype acuity tasks over 8 and 15 weekly sessions, respectively. Participants were masked to the type of vision processing applied in each trial; however, they were aware of the system off condition.

2.8 Statistical Analysis

For the light localization task, descriptive analyses were used to determine the count and percentage of response

accuracy, and to characterize the response time with the number of trials, means and standard error (SEM). These analyses were for each participant (P1 - 3) and vision processing method (i.e., Lanczos2, MVP, system off). Comparisons between participants and vision processing methods for percentage of accurate responses were calculated using χ^2 statistics. Binomial distributions were calculated to determine whether the accuracy rates were significantly better than chance (i.e., 25%) for each vision processing method.

Only P1 completed the gratings and Landolt C visual acuity tasks and as a consequence small sample sizes were obtained. Hence, Wilcoxon Rank-Sum tests were used to determine whether there were differences in the average visual acuity (cpd) scores between Lanczos2 filtering, MVP, WV, scrambled visual representations and system off for the gratings visual acuity task. For the gratings task, descriptive analyses were used to determine the number of trials, mean (cpd) and standard error mean of visual acuity (cpd) and response time for each vision processing method (i.e., Lanczos2, MVP, WV, scrambled, system off).

Similarly for the Landolt C acuity task, Wilcoxon Rank-Sum tests were used to determine possible differences in average visual acuity (logMAR) between Lanczos2 filtering, MVP, and system off. Descriptive analyses were used to determine the number of trials, mean (cpd) and standard error mean of visual acuity (logMAR) and response time for each vision processing method (i.e., Lanczos2, MVP, system off).

Mild transformations (square root) to the data were made when necessary to achieve a normal distribution for further analyses. Windows SPSS v23 (IBM Corporation, Somers, NY) was used for all statistical analyses.

3 Results

3.1 Performance on Light Localization

The data for each participant were analyzed separately given significant differences in performance [$\chi^2(2) = 6.21, p = 0.045$] for percentage of accurate responses. Specifically, χ^2 analyses indicated P1 had a significantly greater percentage of accuracy of responses (see Table 2) than P2 ($p < 0.001$; Figure 6) and P3 ($p < 0.0001$; Figure 6) for both Lanczos2 filtering and MVP.

The response time was recorded for each trial of the light localization task. P1 averaged 5.6 ± 0.37 ($Mean \pm SEM$) seconds (s) while P2 and P3 had a response time of 37.1 ± 3.52s and 50.4 ± 4.19s (see Table 3; Figure 7), respectively.

3.2 The Overall Effectiveness of the Vision Processing Methods and System Off for Light Localization

For Lanczos2 filtering, all three participants (P1, P2, P3) performed significantly better than chance achieving higher percentages of correct responses with 97.50% ($p < .0001$), 71.43% ($p < .0001$), and 66.66% ($p < .0001$), respectively (Table 2; Figure 6). Importantly, the percentages of correct responses were greater than the criterion cut-off of 62.50% (i.e., cut-off for clinical meaningfulness) for Lanczos2 filtering for each participant. All the participants also obtained a significantly higher percentage of correct responses than chance for MVP for light localization with 82.50% ($p < .0001$), 47.92% ($p < .0001$), and 42.50% ($p < .01$), for P1 - 3 respectively. However, only P1 achieved an accuracy rate greater than the criterion cut-off for MVP. All three participants performed at chance when the system was switched off.

Accuracy of response					
	Correct		Incorrect		Total count
Participant	No. Trials	Percent	No. Trials	Percent	
Lanczos2					
1	39	97.50	1	2.50	40
2	40	71.43	16	28.57	56
3	32	66.66	16	33.33	48
Total	111	77.08	33	22.92	144
MVP					
1	33	82.50	7	17.50	40
2	23	47.92	25	52.08	48
3	17	42.50	23	57.50	40
Total	73	57.03	55	42.97	128
System Off					
1	20	27.78	52	72.22	72
2	10	25.00	30	75.00	40
3	10	25.00	30	75.00	40
Total	40	26.32	112	73.68	152

Table 2: Counts and percentages for accuracy of response for the BaLM light localization task (N = 3). No. Trials - Number of light localization trials. Accuracy of response refers to whether the participant was able to correctly identify the location of a wedge of light in relation to the central fixation disc.

3.3 Comparing the Effectiveness of the Vision Processing Methods and System Off for Light Localization

Direct comparisons were made between Lanczos2 filtering, MVP and system off in order to determine differences in performance for light localization. Lanczos2 filtering achieved significantly higher percentages of accuracy than MVP for P1 [$\chi^2(1) = 5.00$, $p = 0.025$], P2 [$\chi^2(1) = 5.98$, $p = 0.014$] and P3 [$\chi^2(1) = 5.16$, $p = 0.023$]. As expected, Lanczos2 filtering was associated with significantly higher percentages of correct responses compared to system off with $p < 0.0001$ for all three participants. MVP performed significantly better than system off for P1 ($p < 0.0001$) and P2 ($p = 0.027$) however, no significant difference in performance between MVP and system off was evident for P3 ($p = 0.098$; Table 2; Figure 6).

The overall average response time for completing the light localization trials was 43.9 ± 3.82s. Specifically, the

Response time(s) for all trials				
		No. Trials	Mean (s)	SEM
Vision Condition	Participant			
Lanczos2	1	32	6.5	0.77
	2	17	45.3	5.62
	3	9	49.4	7.65
	Total	58	24.5	3.34
MVP	1	36	6.0	0.58
	2	11	55.6	4.48
	3	28	72.5	5.95
	Total	75	38.1	4.31
System Off	1	72	5.0	0.57
	2	16	15.6	1.20
	3	24	24.9	2.69
	Total	112	10.8	1.05

Table 3: Counts, means and standard error of mean (SEM) for response time for the BaLM light localization task (N = 3). Response time refers to the time taken to give a response on the location of the wedge of light.

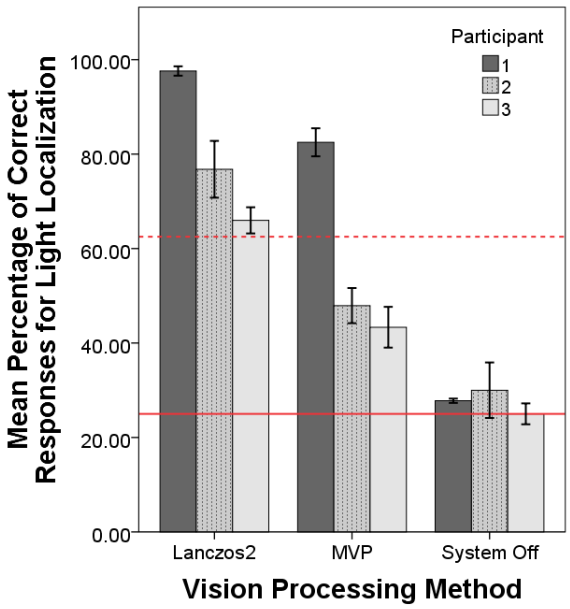

Figure 6: A comparison of the percentage of correct responses for vision processing with each participant (N = 3 participants) for the BaLM light localization task. The error bars represent 95% confidence intervals. The solid horizontal line indicates the level of chance (25.00%) for a correct response, while the dashed horizontal line shows the criterion for success (62.50%).

average response time was 24.5 ± 3.34s for Lanczos2, while MVP and system off had 38.1 ± 4.31s and 10.8 ± 1.05s (see Table 3; Figure 7), respectively.

3.4 Comparing the Effectiveness of the Vision Processing Methods and System Off for Gratings Acuity

Cycles per degree			
Vision Condition	No. Trials	Mean	SEM
Lanczos2	8	0.124	0.004
MVP	4	0.108	0.010
WV	4	0.090	0.007
Scrambled	3	0.030	0.001
System Off	4	0.035	0.005
Total	23	0.087	0.008
Response time(s)			
Vision Condition	No. Trials	Mean (s)	SEM
Lanczos2	8	51.5	3.95
MVP	4	48.4	3.63
WV	4	57.0	5.15
Scrambled	3	54.0	5.52
System Off	4	7.2	1.37
Total	23	44.5	4.09

Table 4: Counts, means, standard error of mean (SEM) for visual acuity (cycles per degree) and Response Time for the gratings visual acuity task (N = 1). Note. No. Trials - Number of gratings visual acuity trials. Response time (recorded for the whole 23 presentations and averaged) refers to the time taken to give a response on the direction of the lines and measured in seconds. Trials were conducted with P1.

Gratings tests were used to compare visual acuity (cpd) scores between Lanczos2 filtering, MVP, WV, scrambled and system off (see Table 4; Figure 8) using Wilcoxon Rank-Sum tests. The non-parametric tests indicated that Lanczos2 filtering ($N = 8$ trials, 0.12 ± 0.004 cpd) and MVP ($N = 4$ trials, 0.11 ± 0.010 cpd) performed similarly ($p = 0.15$) on the gratings acuity task. When compared to WV ($N = 4$ trials, 0.090 ± 0.007 cpd), Lanczos2 filtering was associated with significantly better acuity with $p = 0.004$. As expected, Lanczos2 filtering had significantly better cpd scores compared to scrambled vision processing ($p = 0.012$; $N = 3$ trials, 0.030 ± 0.001 cpd) and when the system was switched off ($p = 0.004$; $N = 4$ trials, 0.040 ± 0.005 cpd). Similarly, MVP was associated with significantly greater accuracy on the gratings task when compared to system off ($p = 0.029$); however, there was no significant difference between MVP and the WV ($p = 0.343$) or scrambled ($p = 0.057$) visual representations for acuity. The WV visual representation did not have significantly better acuity scores than scrambled vision processing ($p = 0.057$) but had greater acuity than when the system was switched off ($p = 0.029$).

The overall average response time for completing the gratings acuity trials was 44.5 ± 4.09s. Specifically, the average response time was 51.5 ± 3.95s for Lanczos2, 48.4 ± 3.63s for MVP, 57.0 ± 5.15s for WV, while scrambled and system off had 54.0 ± 5.52s and 7.2 ± 1.37s, respectively. (see Table 4; Figure 9).

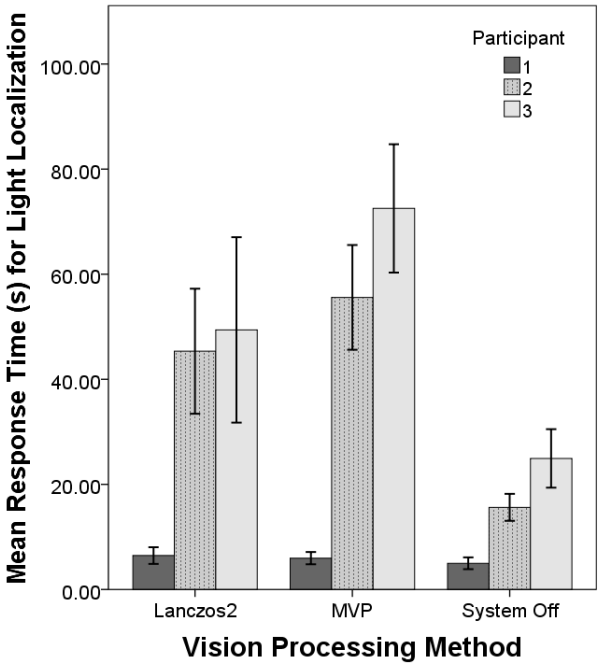

Figure 7: A comparison of the average response time for vision processing with each participant (N = 3 participants) for the BaLM light localization task. The error bars represent 95% confidence intervals.

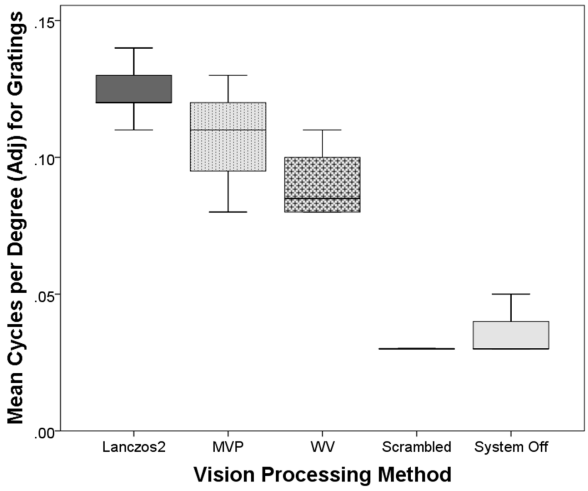

Figure 8: A comparison of the average (mean) cycles per degree for vision processing with P1 for the gratings visual acuity task.

3.5 Comparing the Effectiveness of the Vision Processing Methods and System Off for Landolt C Optotype Acuity

Landolt C optotypes were used to compare visual acuity (mean logMAR) scores between Lanczos2 filtering, MVP and system off (see Table 5 and Figure 10). Lanczos2 filtering ($N = 20$ trials, 2.65 ± 0.044; Figure 10) and MVP ($N = 15$ trials, 2.66 ± 0.033) performed similarly (Wilcoxon Rank-Sum test; $p = 0.805$) on the Landolt C acuity task. Non-parametric tests indicated, as expected, both Lanczos2 filtering ($p = 0.009$) and MVP ($p = 0.015$) had significantly better logMAR scores compared to system off ($N = 2$ trials, 3.24 ± 0.005).

The overall average response time for completing the Landolt C acuity trials was 54.3 ± 2.38s (Table 5). Average response times for Lanczos2 filtering, MVP and system off were 58.2 ± 2.56s, 55.0 ± 2.25s and 11.4 ± 0.21s, respectively. (see Figure 11).

Overall, it is acknowledged that the findings for gratings and Landolt C acuities and response times need to be interpreted with prudence given the small sample size and use of a single participant.

4 Discussion

We presented the first comprehensive report of vision function testing on a 20 electrode retinal prosthesis. Three participants were able to pass a light localization test, and one participant reported acuities on grating and Landolt C tests.

For the first time in implanted participants we demonstrated that appropriate vision processing improves the performance of participants on a light localization task. Specifically that Nyquist bandlimited filtering (Lanczos2) led to higher success rates than MVP and system off. All participants exceeded the criteria for a clinically meaningful result for light localization using Lanczos2 filtering. High quality image filtering was shown to be suitable also for acuity tasks; in a one participant pilot, P1 was able to successfully complete both gratings and Landolt C acuity tests, with mean acuity for gratings of 0.124 cycles per degree (or 2.38 logMAR) and mean acuity for Landolt C of 2.648 logMAR. The grating acuity value is close to the static theoretical expectation for the device based on the electrode spacing on the retina of 2.33 logMAR.

In terms of comparator vision processing methods for the light localization task, only one participant exceeded the criterion for clinical meaningfulness when using MVP. None of the participants performed significantly better than chance in terms of success rate with system off. Further, low acuities were shown for Landolt C and gratings using system off. It is likely that these were not due to perceiving the stimulus but simply due to chance in a 4AFC task. System off performance at chance was expected given the careful screening conducted.

Over all tests, Lanczos2 had equivalent or faster response times to the comparator vision processing methods of WV, MVP and scrambled. In many cases, system off was associated with faster response times than conditions that used vision processing. All participants were generally aware of the system off condition, and so may have responded more rapidly with less accuracy.

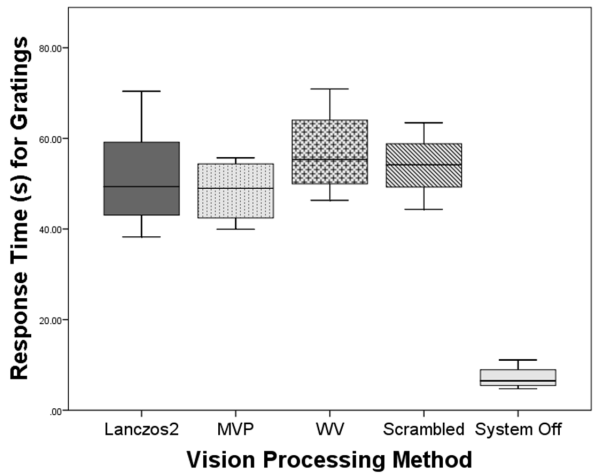

Figure 9: A comparison of the mean response time for vision processing with P1 for the gratings visual acuity task. Response time refers to the time taken to give a response on the direction of the lines and measured in seconds.

logMAR			
Vision Condition	N	Mean	SEM
Lanczos2	20	2.648	0.044
MVP	15	2.662	0.033
System Off	2	3.235	0.007
Total	37	2.685	0.035
Response time(s)			
Vision Condition	N	Mean	SEM
Lanczos2	20	58.2	2.56
MVP	15	55.0	2.25
System Off	2	11.4	0.21
Total	37	54.3	2.38

Table 5: Counts, means, standard error of mean (SEM) for Visual Acuity (logMAR) and Response Time for the Landolt C Optotype Visual Acuity Task in Prosthetic Vision (N = 1). SD - Standard deviation. No. Trials - Number of Landolt C optotype trials. logMAR - Logarithm of the Minimum Angle of Resolution. Response time (measured in seconds) refers to the time taken to give a response on the location of the gap in the C optotype for each trial. Trials were conducted with P1.

P1 was significantly more accurate on both vision processing conditions for light localization than P2 and P3. Further, P1 was able to complete both acuity tasks while neither P2 nor P3 were able to complete the acuity tasks.

This may be due to a large range of factors including: general health status; approach to the task; and, stimulation conditions (P2 and P3 had less phosphenes and required higher stimulation rates). Among these factors, note that P2 and P3 also had Nystagmus which made it difficult for them to maintain central fixation and may have led to eye movements and impacted on the perception of phosphenes even when the head-mounted camera was held still. Note that variation among the performance of participants was also reported by previous studies [1, 13].

Given the number and density of electrodes in this device, the grating acuity value reported in the pilot for P1 falls within the ranges reported across participants in results of previous studies [1, 13]. Humayun *et al.*, [1] report that only 23% of participants were able to achieve a grating acuity between 2.9 and 1.6 logMAR with the best participant achieving 1.8 logMAR, which is better than the static theoretical expectation for their device. Stingl *et al.* [13] reports grating acuities for six out of eight participants, ranging from 0.1 to 3.3 *cpd* with only one participant exceeding the theoretical expectation for the device with 3.3 *cpd*. For the Landolt C acuity test, Stingl *et al.* reports that acuity was assessible in only two out of eight participants, with acuities of 1.43 and 2 logMAR, which are both better than acuities reported in this paper. Landolt C acuity has not been assessed in other human implantee studies. P1 recorded a better acuity score on the gratings tasks than on the Landolt C task, better performance on gratings is consistent with previous findings [13], as above.

The light localization and acuity tasks examined are all 4AFC tests and therefore each only requires the discrimination of four patterns. Further, more general testing is required. Note, however, that participants view the screen-based patterns through a head-mounted camera and did move their heads relative to the screen during trials. As such, this task does not reduce to a task of discriminating four patterns of electrode activations. The electrode activations would change greatly depending on camera pose relative to the screen. Note also that high quality image filtering will lead to a more consistent presentation as the camera moves relative to the screen stimulus.

Lieby *et al.* previously showed that setting the filter size parameter at the Nyquist frequency for Lanczos2 yields the best performance on visual acuity tasks using SPV [24]. The results of the present study appear to support this result, and show evidence for the validity of using simulation to predict relative performance between alternative vision processing methods. The results of the present study are also consistent with other previous SPV studies [22, 23].

4.1 Image filters in implantable prosthetic vision

The results show performance on a 20 stimulating electrode device. To investigate whether this strategy leads to benefits on other devices would require further implanted human studies. However, given the well-understood performance of filtering in image processing, one may reasonably expect filtering to be important for devices with larger numbers of electrodes. SPV with larger numbers of electrodes suggest benefits of image filtering approaches (e.g., [22, 23]).

The participant results of this paper show the value of high quality Nyquist bandlimited filtering for vision processing. In this paper, we only compared the Lanczos2 filter with WV and MVP. It is likely that other other high

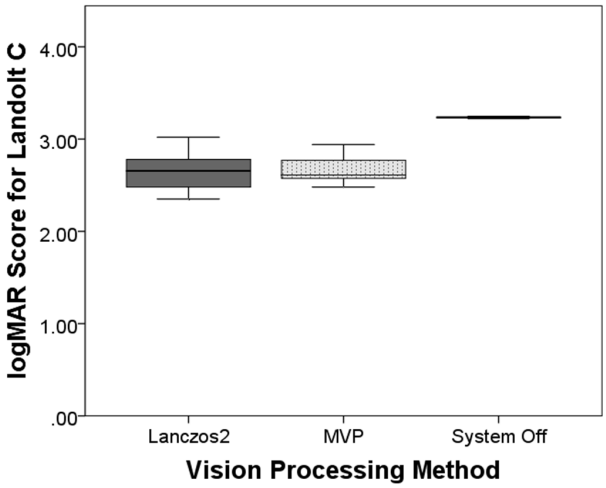

Figure 10: A comparison of the mean logMAR scores for vision processing with P1 for the Landolt C optotype task.

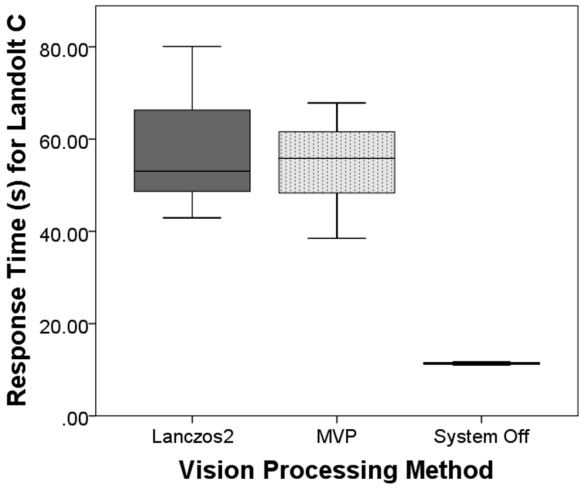

Figure 11: A comparison of the mean response time for vision processing with P1 for the Landolt C optotype task. Response time refers to the time taken to give a response on the location of the gap in the C optotype for each trial.

quality downsampling filters would also lead to improved performance over MVP and WV. In an SPV study, Chen *et al.* [22] reported that setting the filter radius to half the interphosphene distance led to best acuities for regional averaging. It may be expected that the results using regional averaging with this filter size may be better than for that reported for WV. However, in view of the well-understood comparitive performance of these filters we would not expect it to yield better results than the Lanczos2 filter.

In previous work using eye-resident micro-photodiodes [13], the optics of the eye perform filtering of incoming light before sensor acquisition. This work is unlikely to have evaluated Nyquist bandlimited filtering for a retinal prosthetic as the sensor spacing is not at peak foveal density. Also, note that the current micro-photodiode-based device cannot incorporate computational processing such as image filtering. However, as lateral processing has been highlighed as a future concept for the device [2], image filtering may be possible with future devices.

Image filters are a simple and well-established form of image processing, and more advanced vision processing approaches are likely to show advantages. Other challenges for vision processing such as limited ability to perceive noticeable difference using retinal implants (see [2] and [69]) are not addressed by this method. Methods that have shown efficacy in low vision may provide candidate approaches [16], or approaches proposed for specific tasks [28].

4.2 Limitations

In three participants, results only from the light localization task from the BaLM test battery were shown. Pilot data was also shown for a single participant for acuity tasks. In order to fully establish the benefits of vision processing for inplantable prosthetic vision, more extensive vision testing is required. Unfortunately, the total time was limited for the study, and as this is the first chronic implant study of a suprachoroidal device the time available for vision function testing was further restricted. Given time constraints, examining light localization was considered to be the most important subtest of BaLM for this study, with the expectation that determining light localization is an important aspect of general object localization. The motion test was considered less relevant than the localization task as the speed of motion that can be perceived is limited by the working frequency of the device [13]. The effect of image filtering being investigated here is spatial, and so the localization test is the most suitable as it is a spatial test.

5 Conclusion

In this paper we gave a comprehensive report of the vision function testing that was conducted on a suprachoroidal retinal prosthesis, showing that it was effective for restoring aspects of visual function. Three participants were able to pass a light localization test and in a preliminary result, one participant reported acuities on grating and Landolt C tests. Further, for the first time in implanted participants, this study has shown that using appropriate vision processing methods can improve performance of a retinal prosthesis on a localization of light task, improving participant's performance. The method is the Lanczos2 filter with filter size set to remove all frequencies greater than the Nyquist frequency based on the interphosphene distance.

We expect that high quality image filtering will have broad application in prosthetic vision for a range of visual tasks that are important to everyday functioning. This study shows some preliminary evidence that the effectiveness of current retinal prosthetic devices in terms of vision

function can be improved by performing better image preprocessing. In future studies, we will investigate its performance in functional vision tasks including activities of daily living, and orientation and mobility tasks.

Acknowledgments

We thank the participants for their time, involvement and enthusiasm.

We are particularly grateful to Michael Bach for assistance with providing the 'square wave' filter option in the FrACT software for the grating acuity sub-task.

This study was supported by the Australian Research Council through its Special Research Initiative (SRI) in Bionic Vision Science and Technology grant to Bionic Vision Australia (BVA). NICTA is supported by the Australian Government through the Department of Communications and the Australian Research Council through the ICT Centre of Excellence Program. CERA receives Operational Infrastructure Support from the Victorian Government, and is supported by the NH&MRC Centre for Clinical Research Excellence (#529923) Translational Clinical Research in Major Eye Diseases. Bionics Institute receives Operational Infrastructure Support from the Victorian Government.

The BVA Consortium includes: five member organizations NICTA, Centre for Eye Research Australia, Bionics Institute, University of Melbourne, University of New South Wales); and, three partner organizations The Royal Victorian Eye and Ear Hospital, National Vision Research Institute of Australia, University of Western Sydney. For this publication, the consortium members consist of P J Allen, P Blamey, A N Burkitt, O Burns, J Fallon, R H Guymer, C D Luu, D A X Nayagam, R Shepherd, P Seligman, J Villalobos, C Williams, and J Yeoh.

We thank the surgical, clinical, preclinical and psychophysics teams at the Bionics Institute and Centre for Eye Research Australia for their invaluable work in developing and validating the electrode array and patient testing systems used in this study. We also thank all those at NICTA who have contributed to the background work in vision processing towards this study.

Author details

[1]NICTA Computer Vision Research Group, Building A, 7 London Circuit, Canberra, Australia. [2]Research School of Engineering, Australian National University. [3]Centre for Mental Health Research, Australian National University, Canberra, Australia. [4] Bionics Institute, Melbourne, Australia. [5] Centre for Eye Research Australia, University of Melbourne, Royal Victorian Eye and Ear Hospital, Melbourne, Australia. [6] Dept Medical Bionics, University of Melbourne, Melbourne, Australia. [7] School of Software and Electrical Engineering, Swinburne University of Technology, Melbourne, Australia. [8] Graduate School of Biomedical Engineering, University of New South Wales, Melbourne, Australia.

References

1. Humayun M S, Dorn J D, Cruz L D, Dagnelie G, Sachel J A, Stanga P E, Cideciyan A V, Duncan J L, Eliott D, Filley E, Ho A C, Santos A, Safran A B, Arditi A, Del Priore L V, Greenberg R J and for the Argus II Study Group 2012 Interim results from the international trial of second sight's visual prosthesis *Ophthalmology* **119** 779–88
2. Zrenner E, Bartz-Schmidt K, Benav H, Besch D, Bruckmann A, Gabel V P, Gekeler F, Greppaier U, Harscher A, Kibbel S, Kock J, Kusnyerik A, Peters T, Stingl K, Stett A, Szurman P, Wilhelm B and Wilke R 2011 Subretinal electronic chips allow blind patients to read letters and combine them to words *Proc. Royal Society of London B: Biological Sciences* **278** 1489–1497
3. Rizzo III J F, Wyatt J, Loewenstein J, Kelly S and Shire D 2003 Perceptual efficacy of electrical stimulation of human retina with a microelectrode array during short-term surgical trials *Invest. Ophthalmol. and Vis. Sci.* **44** 5995–6003
4. Rizzo III J F 2011 Update on retinal prosthetic research: the Boston retinal implant project *Journal of Neuro-Ophthalmology* **31** 160–8
5. Mokwa W, Goertz M, Koch C, Krisch I, Trieu H and Walter P 2008 Intraocular epiretinal prosthesis to restore vision in blind humans *IEEE Int. Conf. of Eng. in Medicine and Biology Society (EMBC)* pp 5790–3
6. Roessler G, Laube T, Brockmann C, Kirschkamp T, Mazinani B, Goertz M, Koch C, Krisch I, Sellhaus B, Trieu H K, Weis J, Bornfeld N, Rothgen H, Messner A, Mokwa W and Walter P 2009 Implantation and explantation of a wireless epiretinal retina implant device: Observations during the epiret3 prospective clinical trial *Invest. Ophthalmol. and Vis. Sci.* **50** 3003–8
7. Delbeke J, Oozeer M and Veraart C 2003 Position, size and luminosity of phosphenes generated by direct optic nerve stimulation *Vis. Res.* **43** 1091–1102
8. Veraart C, Wanet-Defalque M, Gerard B, Vanlierde A and Delbeke J 2003 Pattern recognition with the optic nerve visual prosthesis *Artif. Organs* **27** 996–1004
9. Panetsos F, Sanchez-Jimenez A, Diaz de Cerio E, Diaz-Guemes I and Sanchez F 2011 Consistent phosphenes generated by electrical microstimulation of the visual thalamus. an experimental approach for thalamic visual neuroprostheses. *Frontiers in Neuroscience* **5** 1–12
10. Pezaris J and Reid R 2007 Demonstration of artificial visual percepts generated through thalamic microstimulation *Proceedings of the National Academy of Sciences* **104** 7670–7675
11. Brindley G S and Lewin W S 1968 The sensations produced by electrical stimulation of the visual cortex *J. Physiology* **196** 479–493
12. Deisseroth K 2011 Optogenetics *Nature Methods* **8** 26–29
13. Stingl K, Bartz-Schmidt K, Besch D, Braun A, Bruckmann A, Gekeler F, Greppmaier U, Hipp S, Hortdorfer G, Kernstock C, Koitschev A, Kusnyerik A, Sachs H, Schatz A, Stingl K T, Wilhelm T P B and Zrenner E 2013 Artificial vision with wirelessly powered subretinal electronic implant alpha-ims *Proc. Royal Society of London B: Biological Sciences* **280**
14. Ayton L N, Blamey P J, Guymer R H, Luu C D, Nayagam D A X, Sinclair N C, Shivdasini M N, Yeoh J, McCombe M F, Briggs R J, Opie N L, Villabos J, Dimitrov P N, Varsamidis M, Petoe M A, McCarthy C D, Walker J G, Barnes N, Burkitt A N, Williams C E, Shepherd R K, Allen P J and the Bionic Vision Australia Consortium 2014 First-in-human trial of a novel suprachoroidal retinal prosthesis *PLOS ONE* **9**
15. Baker S and Kanade T 2002 Limits on super-resolution and how to break them *IEEE Trans. on Pattern Analysis and Machine Intelligence* **24** 1167–1183
16. Peli E, Goldstein R B, Trempe C L and Buzney S M 1991 Image enhancement for the visually impaired: Simulations and result *Invest. Ophthalmol. and Vis. Sci.* **32** 2337–50
17. Luo G and Peli E 2006 Use of an augmented-vision device for visual search by patients with tunnel vision *Invest. Ophthalmol. and Vis. Sci.* **47** 4152–9
18. Peli E, Lee E, Trempe C L and Buzney S 1994 Image enhancement for the visually impaired: the effects of ehancment on face recognition *Jour. Optical Society of America A* **11** 1929–39
19. Al-Atabany W, Memon M A, Downes S M and Degenaar P 2010 Designing and testing scene enhancement algorithms for patients with retina degenerative disorders *Biomedical Engineering Online* **9**
20. Chen S C, Suaning G J, Morley J W and Lovell N H 2009 Simulating prosthetic vision: 1 visual models of phosphenes *Vis. Res.* **49** 1493–1506 dOI:10.1016/j.visres.2009.02.003
21. Chen S C, Lovell N H and Suaning G J 2004 Effect of prosthetic visual by filtering schemes, filter cut-off frequency and phosphene matrix: A virtual reality simulation *IEEE Int. Conf. of Eng. in Medicine and Biology Society (EMBC)*

22. Chen S C, Hallum L E, Lovell N H and Suaning G J 2005 Visual acuity measurement of prosthetic vision: A virtual-reality simulation study *J Neural Eng.* **2** S134–45
23. Hallum L E, Suaning G J, Taubman D S and Lovell N H 2005 Simulated prosthetic visual fixation, saccade, and smooth pursuit *Vis. Res.* **45** 775–788
24. Lieby P, Barnes N, Walker J G, Scott A F and Ayton L 2013 Evaluating Lanczos2 image filtering for visual acuity in simulated prosthetic vision *ARVO*
25. Parikh N, Itti L and Weiland J 2010 Saliency-based image processing for retinal prosthesis *J Neural Eng.* **7** 1–10
26. He X, Kim J and Barnes N 2012 An face-based visual fixation system for prosthetic vision *IEEE Int. Conf. of Eng. in Medicine and Biology Society (EMBC)*
27. Weiland J D, Parikh N, Pradeep V and Medioni G 2012 Smart image processing system for retinal prosthesis *IEEE Int. Conf. of Eng. in Medicine and Biology Society (EMBC)* pp 300–303
28. McCarthy C, Walker J G, Lieby P, Scott A F and Barnes N 2015 Mobility and low contrast trip hazard avoidance using augmented depth *J Neural Eng.* **12**
29. Eckmiller R, Neumann D and Baruth O 2005 Tunable retina encoders for retina implants: why and how *J Neural Eng.* **2** s91–S104
30. Cha K, Horch K and Normann R 1992 Simulation of a phosphene-based visual field: Visual acuity in a pixelized vision system *Annals of Biomedical Engineering* **20** 439–449
31. Hayes J S, Yin V T, Piyathaisere D, Weiland J D, Humayun M S and Dagnelie G 2003 Visually guided performance of simple tasks using simulated proshetic vision *Artif. Organs* **27** 1016–28
32. Cha K, Horch K and Normann R 1992 Mobility performance with a pixelized vision system *Vis. Res.* **32** 1367–1372
33. Humayun M S 2001 Interocular retinal prosthesis *Trans Am Ophthalmological Society* **99** 271–300
34. Jr R W T, Barnett G D, Humayun M S and Dagnelie G 2003 Facial recognition using simulated prosthetic pixelized vision *Invest. Ophthalmol. and Vis. Sci.* **44** 5035–42
35. Williams D R and Hofer H 2004 *The Visual Neurosciences: Volume 1* (Cambridge Massachusetts: MIT Press) chap Formation and Acquisition of the Retinal Image, pp 795–810
36. Hallum L E, Cloherty S L and Lovell N H 2008 Image analysis for microelectric retinal prosthesis *IEEE Trans. Biomed. Eng.* **55** 344–346
37. Humayun M, Dorn J D, Ahuja A K, Caspi A, Filley E, Dagnelie G, Salzmann J, Santos A, Duncan J, daCruz L, Mohand-Said S, Eliott D, McMahon M J and Greenberg R J 2009 Preliminary 6 month results from the argus ii epiretinal prosthesis feasibility study *IEEE Int. Conf. of Eng. in Medicine and Biology Society (EMBC)* pp 4566–4568
38. Stanga P E, Sahel J A, Mohand-Said S, daCruz L, Merlini A C F, Greenberg R J and Group A I S 2013 Face detection using the Argus(R) II retinal prosthesis system *ARVO*
39. Sahel J A, Mohand-Said S, Stanga P E, Caspi A and Greenberg R J 2013 Acuboost: Enhancing the maximum acuity of the Argus II retinal prosthesis system *ARVO*
40. Oppenheim A V, Schafer R W and Buck J R 1999 *Discrete-time signal processing : Second Edition* (New Jersey: Prentice Hall)
41. Gonzalez R C and Woods R E 2002 *Digital Image Processing : Second Edition* (New Jersey: Prentice Hall)
42. Meijering E H W, Niessen W J, Pluim J P W and Viergever M A 1999 Quantitative comparison of sinc-approximating kernels for medical image interpolation *LNCS 1679, MICCAI* pp 210–217
43. Ayton L N, Apollo N V, Varsamidis M, Dimitrov P N, Guymer R H and Luu C D 2014 Assessment of residual visual function in severe vision loss. *Invest. Ophthalmol. and Vis. Sci.* **55** 1332–8
44. Villalobos J, Nayagam D A, Allen P J, Luu C D, Ayton L N, Freemantle A L, McPhedran M, Basa M, McGowan C C, Shepherd R K and Williams C E 2013 A wide-field suprachoroidal retinal prosthesis is stable and well tolerated following chronic implantation. *Invest. Ophthalmol. and Vis. Sci.* **54** 3751–62
45. Saunders A L, Williams C E and and W H 2014 Development of a surgical proceedure for implantation of a prototype suprachoroidal retinal prosthesis. *Clin. Exp. Ophthalmol.* **42** 665–74
46. Slater K D, Sinclair N C, Nelson T S, Blamey P J and McDermott H J 2015 A highly configurable neurostimulator for a retinal prosthesis and other applications *IEEE J. Translational Eng. in Health and Medicine* **3** 1–11
47. Horsager A and Fine I 2011 The perceptual effects of chronic retinal stimulation *Visual Prosthetics* ed Dagnelie G (New York, US: Springer) pp 271–300
48. Stronks H C and Dagnelie G 2011 Phosphene mapping techniques for visual prostheses *Visual Prosthetics* ed Dagnelie G (New York, US: Springer) pp 367–383
49. Eckmiller R, Baruth O and Neumann D 2004 Neural information processing efforts to restore vision in the blind *Advances in Neural Information Processing Systems (NIPS) 16*
50. Dacey D M and Petersen M R 1992 Dendritic field size and morphology of midget and parasol ganglion cells of the human retina *Proceedings of the National Academy of Sciences* **89** 9666–70
51. Shivdasini M N, Sinclair N C, Dimitrov P N, Varsamidis M, Ayton L N, Perera T, McDermott H J and Blamey P J 2013 Factors affecting perceptual thresholds in a suprachoroidal retinal prosthesis *Invest. Ophthalmol. and Vis. Sci.* **55** 6467–6481
52. Merrill D R and Tresco P A 2005 Impedance characterization of microarray recording electrodes in vitro *IEEE Trans. Biomed. Eng.* **52** 1960–5
53. Perez Fornos A, Sommerhalder J, da Cruz L, Sahel J A, Mohnand-Said S, Hafezi F and Pelizzone M 2012 Temporal properties of visual perception on electrical stimulation of the retina *Invest. Ophthalmol. and Vis. Sci.* **53** 2720–31
54. Ray A, Lee E J, Humayun M S and Weiland J D 2011 Continuous electrical stimulation decreases retinal excitability but does not alter retinal morphology *J Neural Eng.* **8**
55. Whitehead N and Fit-Florea A 2011 Precision & performance: Floating point and ieee 754 compliance for nvidia gpus *nVidia technical white paper*
56. Wikipedia 2004 Arm architecture [Online; accessed 19-Nov-2015] URL `https:en.wikipedia.orgwikiARM_architecture`
57. Douchon C E 1979 Lanczos filtering in one and two dimensions *Journal of Applied Meterology* **18** 1016–1022
58. Turkowski K 1990 Filters for common resampling tasks *Graphics Gems* ed Glassner A S (Cambridge: Academic Press) pp 147–165
59. Mitchell D P and Netravali A N 1988 Reconstruction filters in computer graphics *ACM Computer Graphics* **27** 221–228
60. Smith S W 2003 *Digital Signal Processing: A Practical Guide for Engineers and Scientists* (Burlington, MA, USA: Newnes)
61. Caspi A, Dorn J D, Kelly H, MClure M S, Humayun M D, Greenberg R J and McMahon M J 2009 Feasibility study of a retinal prosthesis spatial vision with a 16-electrode implant *JAMA Ophthalmology* **127** 398–401
62. Dorn J D, Ahuja A K, Caspi A, daCruz L, Dagnellie G, Sahel J A, Greenberg R J and McMahon M J 2013 The detection of motion by blind subjects with the epiretinal 60-electrode (Argus II) retinal prosthesis *JAMA Ophthalmology* **131** 183–189
63. Bach M, Wilke M, Wilhelm B, Zrenner E and Wilke R 2010 Basic quantitative assessment of visual performance in patients with very low vision *Invest. Ophthalmol. and Vis. Sci.* **51** 1255–1260
64. Bach M 1996 The “freiburg visual acuity test” - automatic measurement of visual acuity *Optometry and Vision Science* **73** 49–63
65. Bach M Frieburg Vision Test (FrACT) `http://www.michaelbach.de/fract/index.htm` accessed: 2013
66. Pentland A P 1980 Maximum likelihood estimation: The best PEST *Perception and Pscyhophysics* **28** 377–379
67. Wilke R, Bach M, Wilheml B, Durst W, Trauzettel-Klosinski S and Zrenner E 2008 *Artificial Sight* (New York: Springer) chap Testing visual functions in patients with visual prostheses, pp 91–110
68. Nau A, Bach M and Fisher C 2013 Clinical tests of ultra-low vision used to evaluate rudimentary visual perceptions enabled by the brainport vision device *Translational Vision Science and Technology* **2** 1–12
69. Humayun M S, Weiland J, Fujii G Y, Greenberg R, Williamson R, Little J, Mech B, Cimmarusti V, Boemel G V, Dagnelie G and deJuan E 2003 Visual perception in a blind subject with a chronic microelectronic retinal prosthesis *Vis. Res.* **43** 2573–2585